Modelling of linearized Zoeppritz approximations

Arnim B. Haase

ABSTRACT

The Aki and Richards approximations to Zoeppritz's equations as well as approximations by Stewart, Smith and Gidlow, and Fatti et al. are employed to compute AVO-responses of two-layer models for AVO-Classes 1 through 4. These approximate responses are compared to exact Zoeppritz. A weak reflector and a strong reflector are considered for all AVO-Classes in order to test the small parameter change assumption. It is found that these approximations are not always close to exact Zoeppritz at small angles. Neither are these approximations always more accurate for weaker reflectors than they are for strong reflectors.

INTRODUCTION

Zoeppritz's equations completely determine amplitudes of reflected and transmitted plane waves at a planar boundary of two elastic media in welded contact for all incidence angles. In order to gain more insight into the factors that control amplitude changes with angle/offset, and simplify computations, linearized approximations to the Zoeppritz equations have been developed. Aki and Richards (1980) introduce a three term approximation for R_{pp}. Smith and Gidlow (1987) make use of Gardner's relation between density and P-wave velocity in order to eliminate density from the Aki and Richards approximation to Zoeppritz. Fatti et al. (1994) rewrite the Aki and Richards approximate equation for R_{pp} in terms of acoustic impedances. They arrive at their final equation by dropping some density terms, thereby making a small angle assumption. Aki and Richards (1980) also introduce an approximation for converted wave reflection coefficients R_{ps}. Stewart (1990) derives a modified equation for R_{ps} by using Gardner's relation in order to eliminate density from Aki and Richards's equation for R_{ps}.

In general, these approximations assume small elastic parameter changes across the interface. They are said to break down at incidence angles beyond 30 degrees. These limitations do not exist for the exact Zoeppritz equations; however, even "exact Zoeppritz" is a plane wave approximation to the real world.

The purpose of this modelling study is to compare exact AVO-responses for Classes 1 through 4 with the approximations listed above.

REVIEW OF THE INTRODUCED LINEARIZED APPROXIMATIONS

The Aki and Richards approximations to Zoeppritz's equations (Aki and Richards, 1980, page 153) for R_{pp} and R_{ps} are

$$R_{pp}(\theta) \approx \frac{1}{2}(1-4\frac{\beta^2}{\alpha^2}\sin^2\theta)\frac{\triangle\rho}{\rho}+\frac{1}{2}(1+\tan^2\theta)\frac{\triangle\alpha}{\alpha}-4\frac{\beta^2}{\alpha^2}\sin^2\theta\frac{\triangle\beta}{\beta}, \qquad (1)$$

and

$$R_{ps}(\theta) \approx -\frac{1}{2}\tan\varphi\left[\left(\frac{\alpha}{\beta} - 2\frac{\beta}{\alpha}\sin^2\theta + 2\cos\theta\cos\varphi\right)\frac{\Delta\rho}{\rho} - 4\left(\frac{\beta}{\alpha}\sin^2\theta - \cos\theta\cos\varphi\right)\frac{\Delta\beta}{\beta} \right], \tag{2}$$

where R_{pp} is the P-wave reflection coefficient, R_{ps} is the C-wave reflection coefficient, α, β, ρ are the average P-wave and S-wave velocities, and densities across the interface, $\Delta\alpha$, $\Delta\beta$, $\Delta\rho$ are the parameter changes across the interface, θ is the average of θ_1 and θ_2 (P-wave incidence and transmission angles), and φ is the average of φ_1 and φ_2 (S-wave reflection and transmission angles).

When eliminating density ρ by applying Gardner's relation to Equation 1, Smith and Gidlow (1987) obtain the approximation

$$R_{pp}(\theta) \approx \frac{5}{8}\frac{\Delta\alpha}{\alpha} - \frac{\beta^2}{\alpha^2}\left(4\frac{\Delta\beta}{\beta} + \frac{\Delta\alpha}{2\alpha}\right)\sin^2\theta + \frac{\Delta\alpha}{2\alpha}\tan^2\theta\,. \tag{3}$$

Also starting from Equation 1, Fatti et al. (1994) neglect some density terms and arrive at

$$R_{pp}(\theta) \approx \frac{\Delta I}{I}(1 + \tan^2\theta) - 4\frac{\beta^2}{\alpha^2}\frac{\Delta J}{J}\sin^2\theta\,, \tag{4}$$

where $\Delta I/I = \Delta\alpha/\alpha + \Delta\rho/\rho$ and $\Delta J/J = \Delta\beta/\beta + \Delta\rho/\rho$. $\Delta I/I$ is the P-wave zero offset reflection coefficient and $\Delta J/J$ is the S-wave zero offset reflection coefficient.

Stewart (1990) applies Gardner's relation to both Equations 1 and 2. For R_{ps} he obtains

$$R_{ps}(\theta) \approx -\frac{\Delta\alpha}{8\beta}\tan\varphi\left(1 - 2\frac{\beta^2}{\alpha^2}\sin^2\theta + 2\frac{\beta}{\alpha}\cos\theta\cos\varphi\right) + 2\frac{\Delta\beta}{\beta}\tan\varphi\left(\frac{\beta}{\alpha}\sin^2\theta - \cos\theta\cos\varphi\right) \tag{5}$$

MODELLING OF APPROXIMATION ERRORS

Table 1 (taken from Haase and Ursenbach, 2004) repeats layer parameters for two-layer AVO-models adapted from Rutherford and Williams (1989) for Classes 1, 2 and 3, and from Castagna et al. (1998) for Class 4.

Table 1. Layer Parameters for weak reflectors.

Class	α_1/[m/s]	β_1/[m/s]	ρ_1/[kg/m^3]	α_2/[m/s]	β_2/[m/s]	ρ_2/[kg/m^3]
1	2000	879.88	2400	2933.33	1882.29	2000
2	2000	879.88	2400	2400	1540.05	2000
3	2000	879.88	2400	1963.64	1260.04	2000
4	2000	1000	2400	1598.77	654.32	2456.43

The layer parameters listed in Table 2 are selected for larger reflection coefficients to allow testing of the small parameter change assumption. The Class 1 model is adapted from Krail and Brysk (1983) with $R_{pp}(0)$ = 0.38. For the Class 2 model $R_{pp}(0)$ is set to zero. A large parameter change is selected by setting $R_{ss}(0) = 0.359$ in an adaptation of the Class 2 example given by Rutherford and Williams (1989). The Class 3 model is based on Ostrander (1984) with $R_{pp} = -0.365$. Class 4 is adapted from Castagna et al. (1998) as before; $R_{pp}(0)$ is set to -0.379 in this case.

Table 2. Layer Parameters for strong reflectors.

Class	α_1/[m/s]	β_1/[m/s]	ρ_1/[kg/m^3]	α_2/[m/s]	β_2/[m/s]	ρ_2/[kg/m^3]
1	2000	1155	2400	4000	2309	2667
2	2000	666.7	2400	2400	1697	2000
3	2200	898.2	2500	1500	1000	1705
4	3240	1620	2340	1650	1090	2070

AVO-responses are computed with the linearized Zoeppritz approximations reviewed in the foregoing. Exact plane wave responses computed with Zoeppritz's equations are added to the displays for comparison. Figures 1a through 8a show C-wave AVO-responses for Aki and Richards's approximation, Stewart's approximation, and true Zoeppritz. Figures 1b through 8b give P-wave AVO-responses for Aki and Richards's approximation, Smith and Gidlow's approximation, the approximation introduced by Fatti et al., and true Zoeppritz.

DISCUSSION AND CONCLUSIONS

Class 1 AVO-responses for the weaker reflector are compared in Figures 1a and 1b. There is a significant departure of all three P-wave approximations from exact Zoeppritz even below 20 degrees of angle. Approximations are said to degrade near the critical point and at large angles. However, Figures 1 through 4 show reasonable responses near critical angles.

The large parameter change cases of Class 1 are given in Figures 2a and 2b. Again, there is a significant departure from exact Zoeppritz even below 20 degrees of angle. Surprisingly, the relative P-wave departure appears to be less for the $R_{pp}(0) = 0.38$ case when compared to the $R_{pp}(0) = 0.1$ case of the weaker reflector.

Figures 3 and 4 show the corresponding Class 2 examples. The P-wave response of Class 2 is very similar to Class 1. However, the C-wave response of Class 2 shows much better agreement with exact Zoeppritz below 15 degrees of angle than does Class 1.

Class 3 AVO-responses are given in Figures 5 and 6. For P-waves, the Aki and Richards as well as the Fatti et al. approximations are quite close to exact Zoeppritz below about 40 degrees. For C-waves, the Aki and Richards approximation is close to exact Zoeppritz below about 20 degrees of angle for the strong reflector, but not for the weak reflector comparison. This, again, is surprising. Note that there is no critical angle in Class 3 and 4 cases because of P-wave velocity inversions.

Figures 7 and 8 display Class 4 responses. Except for the Smith and Gidlow approximation, all approximations are quite close to exact Zoeppritz at small angles. This is similar to Class 3 P-wave responses. Even at large angles, the departure from exact Zoeppritz is much smaller for all Class 4 examples when compared to Class 3 responses.

Except for Class 4 C-waves, the approximations with Gardner's relation (Smith and Gidlow as well as Stewart) depart the most from exact Zoeppritz at small to intermediate angles. A quick calculation for the layer parameters given in Tables 1 and 2 reveals that only for the large parameter change cases of Classes 1 and 4 is Gardner's relation appropriate.

REFERENCES

Aki, K.T., and Richards, P.G., 1980, Quantitative Seismology: Theory and Methods: Vol. 1, W.H. Freeman and Co.

Castagna, J.P., Swan, H.W., and Foster, D.J., 1998, Framework for AVO gradient and intercept interpretation: Geophysics, **63**, 948-956.

Fatti, J.L., Smith, G.C., Vail, P.J., Strauss, P.J., and Levitt, P.R., 1994, Detection of gas in sandstone reservoirs using AVO analysis: A 3-D seismic case history using the Geostack technique: Geophysics, **59**, 1362-1376.

Haase, A.B., and Ursenbach, C.P., 2004, Spherical wave AVO-modelling in elastic isotropic media: CREWES Research Report, **16**.

Krail, P.M., and Brysk, H., 1983, Reflection of spherical seismic waves in elastic layered media: Geophysics, **48**, 655-664.

Ostrander, W.J., 1984, Plane-wave reflection coefficients for gas sands at nonnormal angles of incidence: Geophysics, **49**, 1637-1648.

Rutherford, S.R., and Williams, R.H., 1989, Amplitude-versus-offset variations in gas sands: Geophysics, **54**, 680-688.

Smith, G.C., and Gidlow, P.M., 1987, Weighted Stacking for Rock Property Estimation and Detection of Gas: Geophysical Prospecting, **35**, 993-1014.

Stewart, R.R., 1990, Joint P and P-SV Inversion: CREWES Research Report, **2**.

ACKNOWLEDGEMENTS

The author wishes to thank the sponsors of CREWES for their financial support.

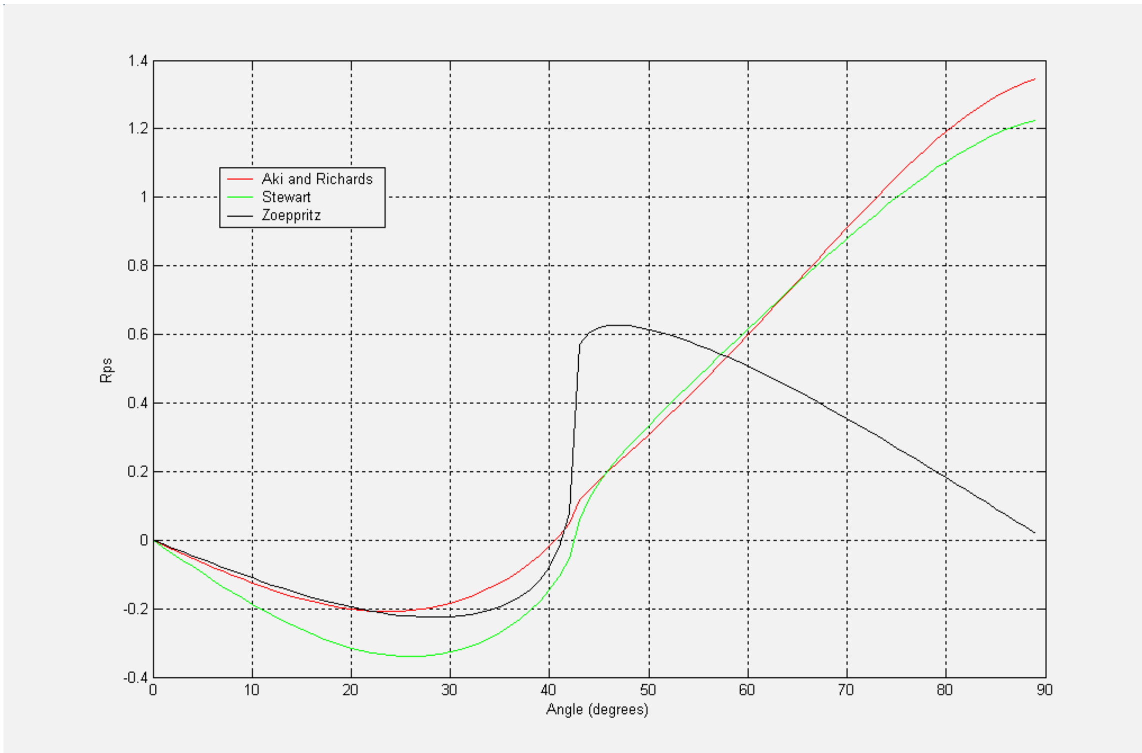

FIG. 1a. Class 1 (weak) R_{ps}.

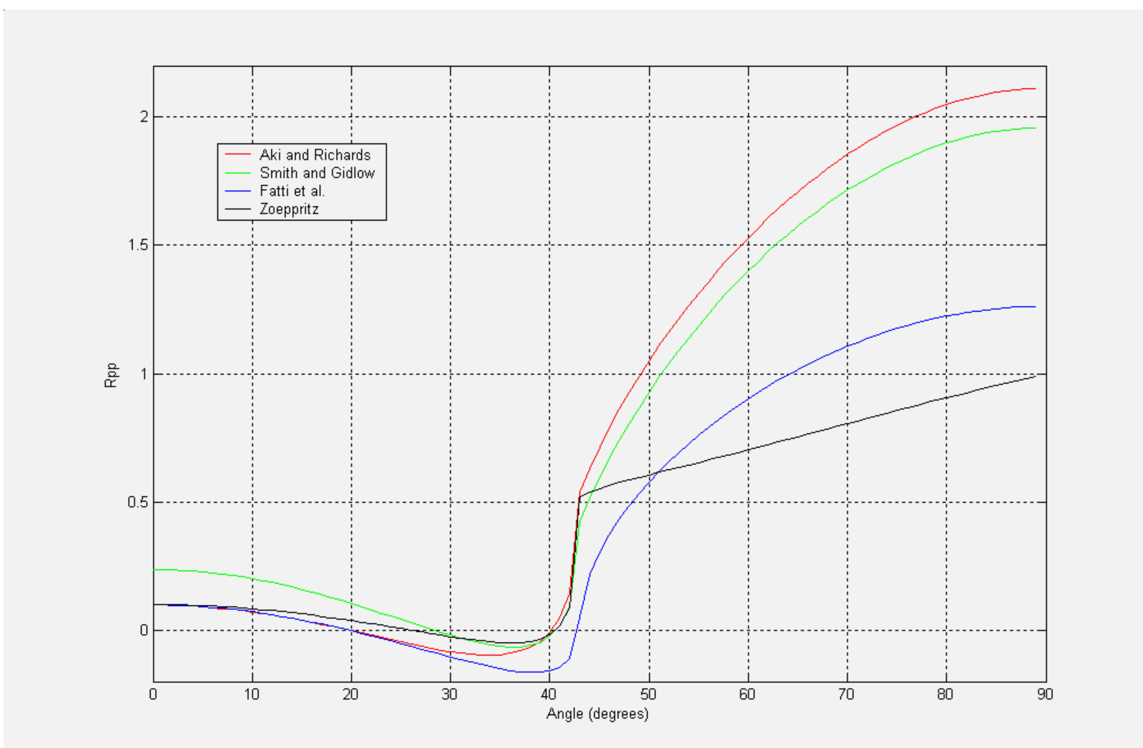

FIG. 1b. Class 1 (weak) R_{pp}.

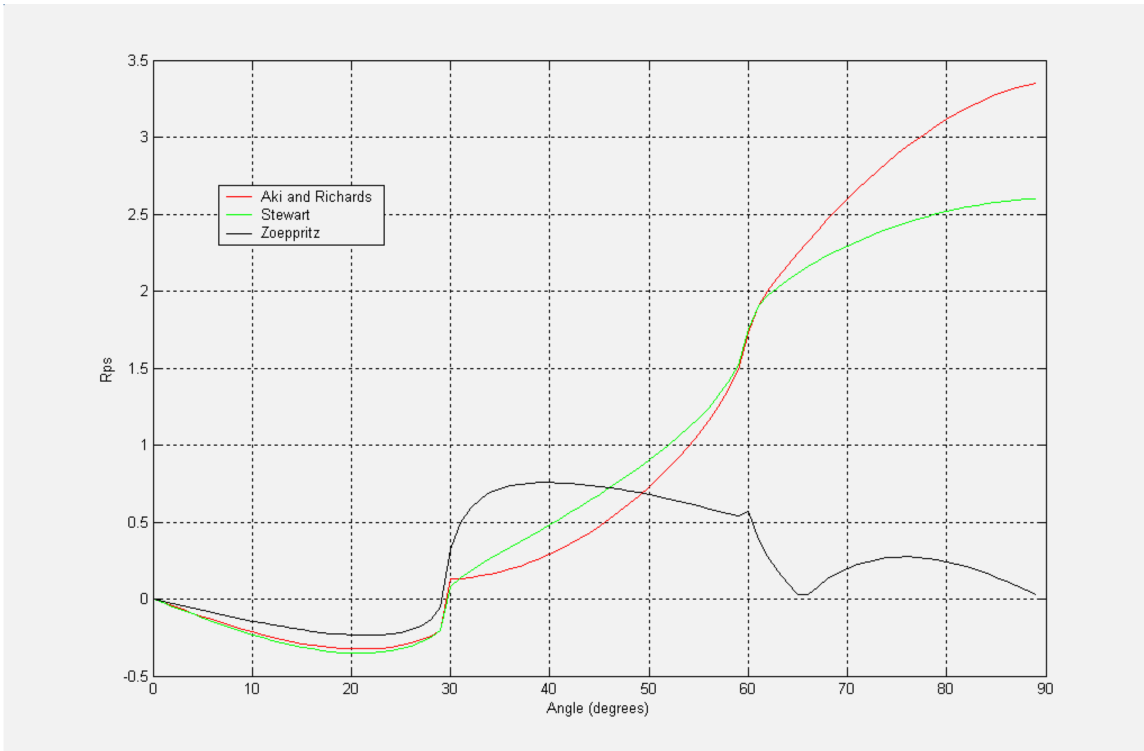

FIG. 2a. Class 1 (strong) R_{ps}.

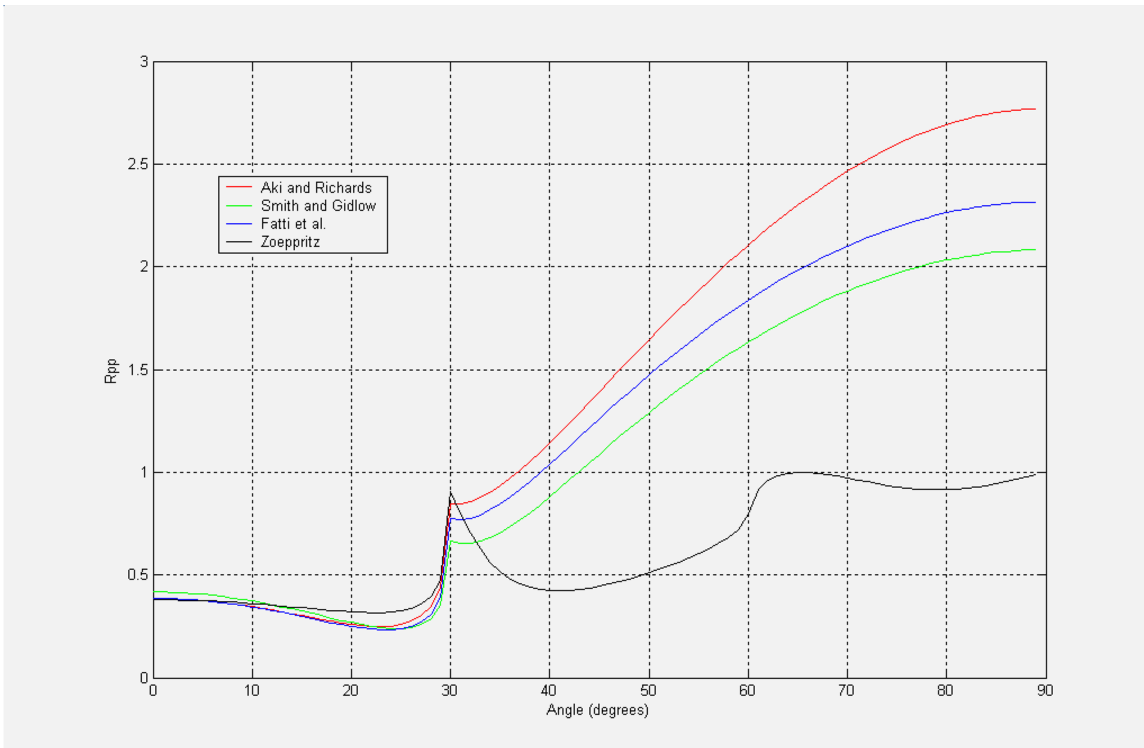

FIG. 2b. Class 1 (strong) R_{pp}.

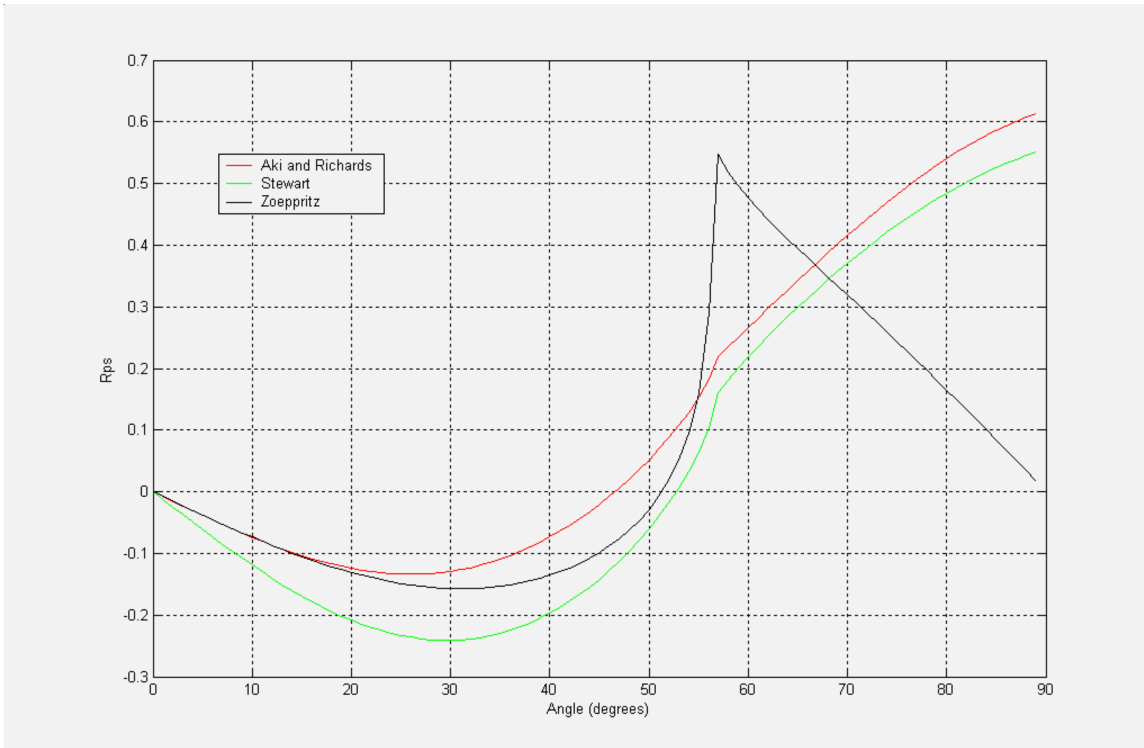

FIG. 3a. Class 2 (weak) R_{ps}.

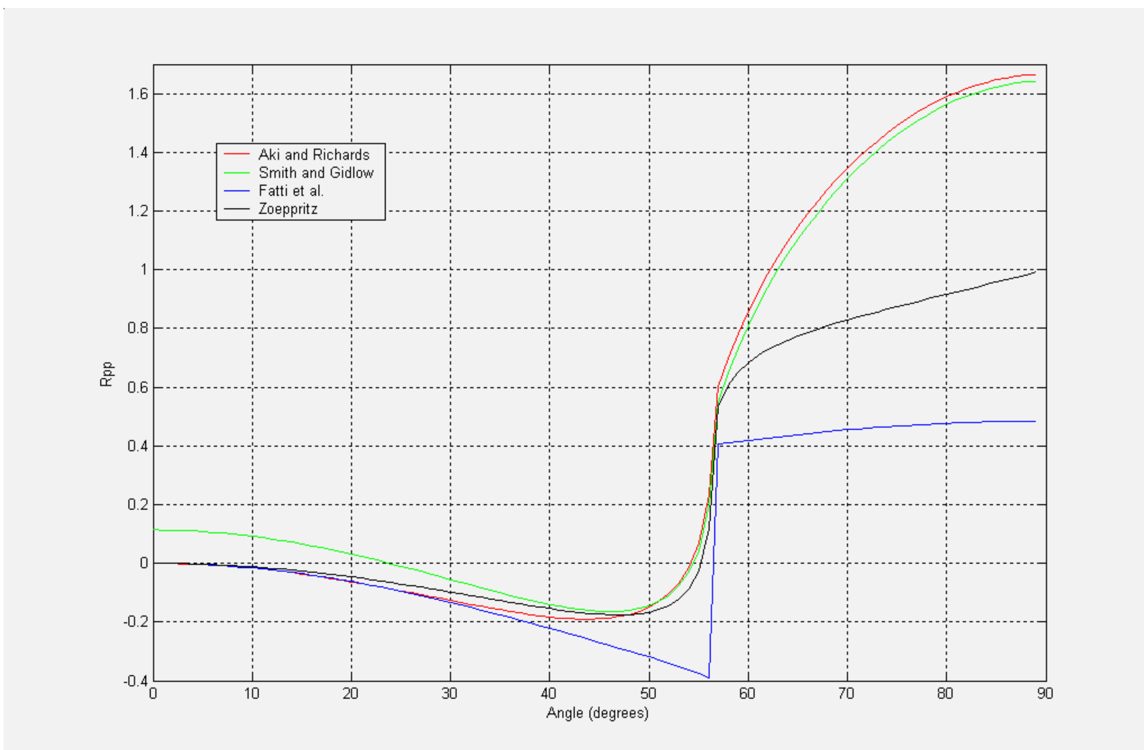

FIG. 3b. Class 2 (weak) R_{pp}.

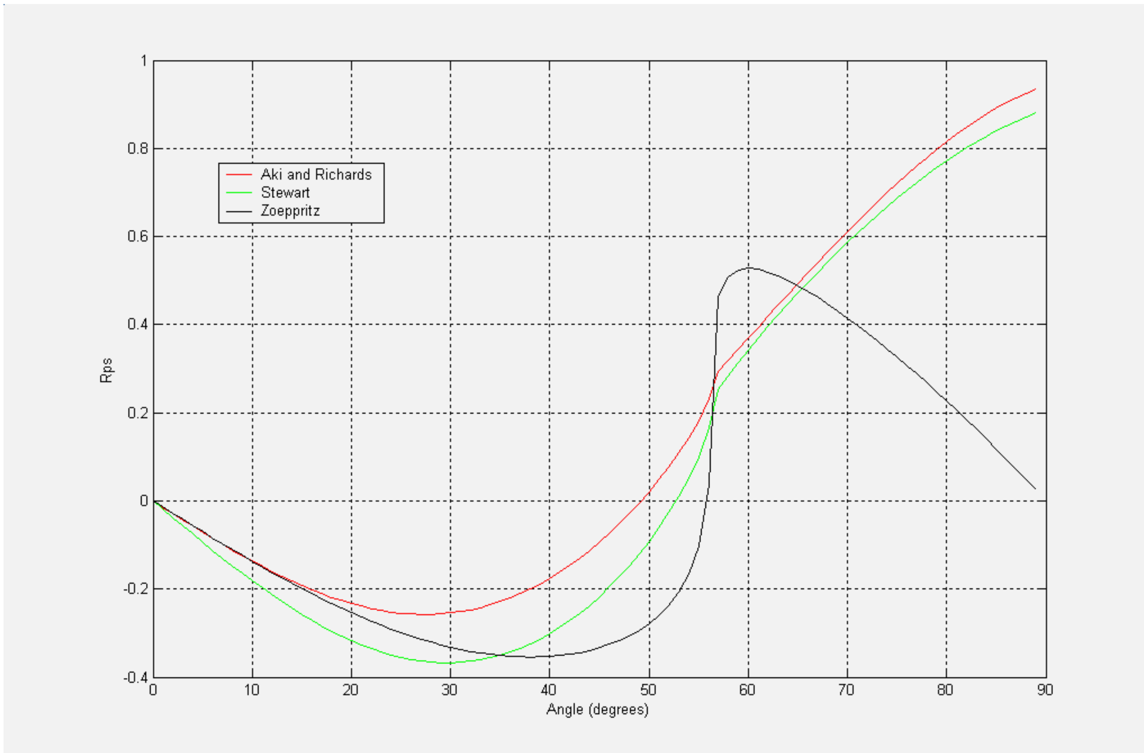

FIG. 4a. Class 2 (strong) R_{ps}.

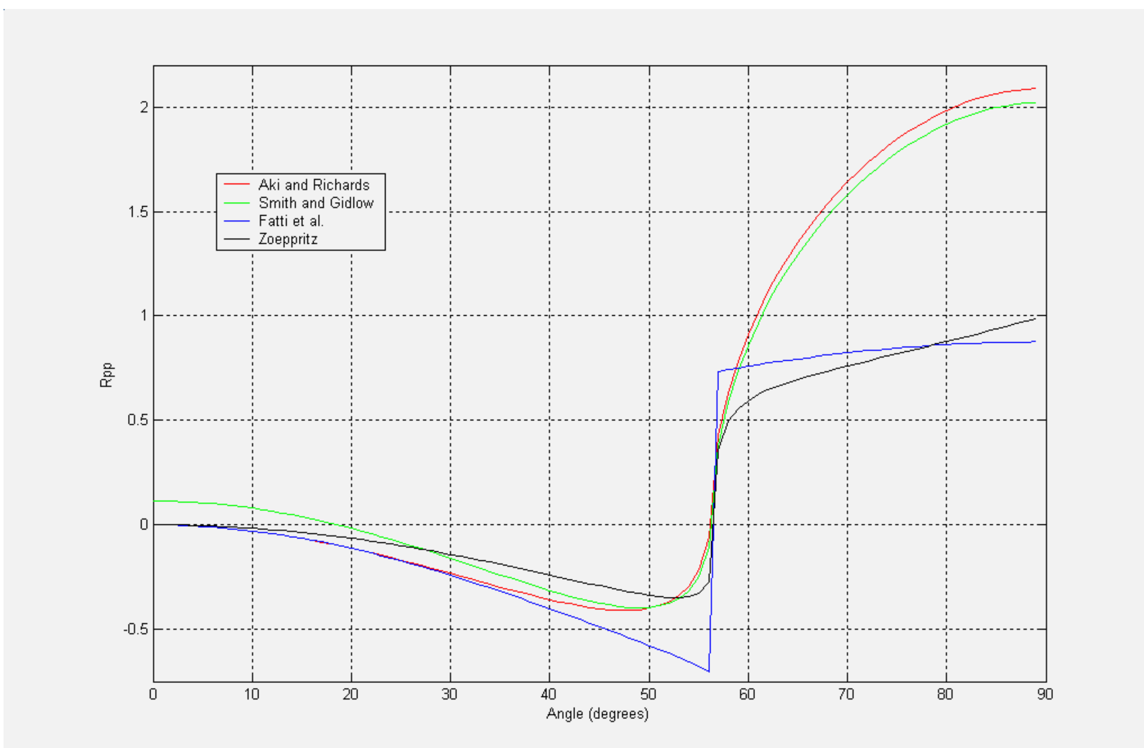

FIG. 4b. Class 2 (strong) R_{pp}.

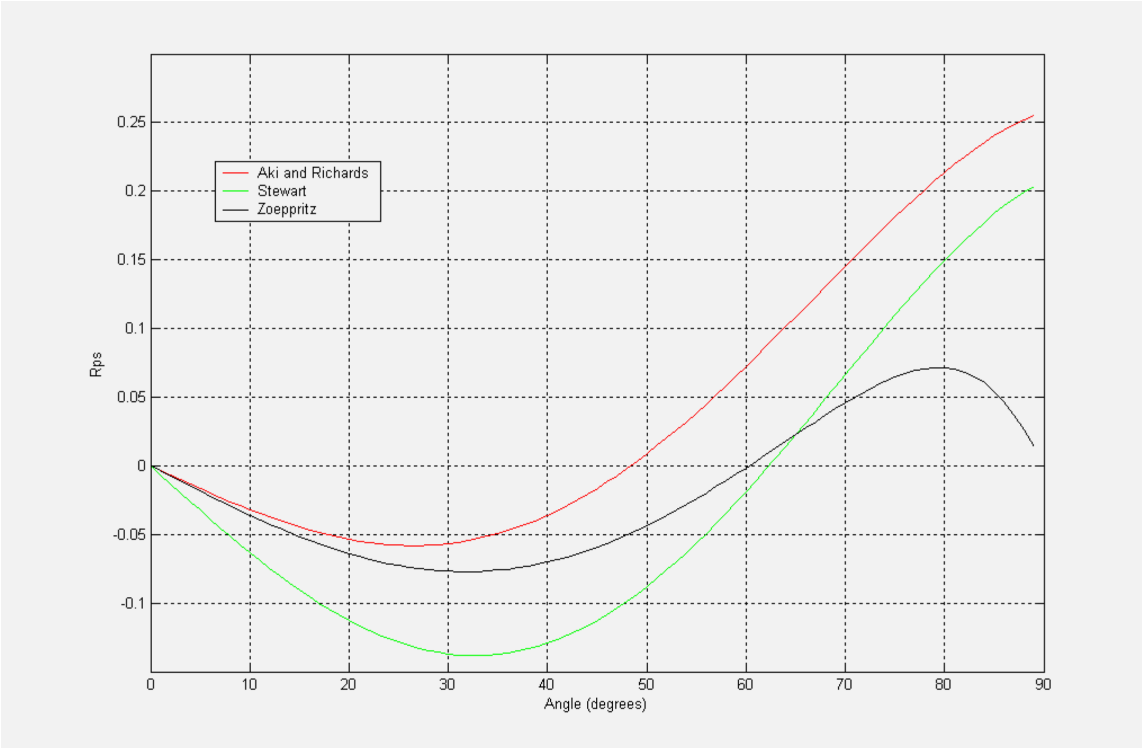

FIG. 5a. Class 3 (weak) R_{ps}.

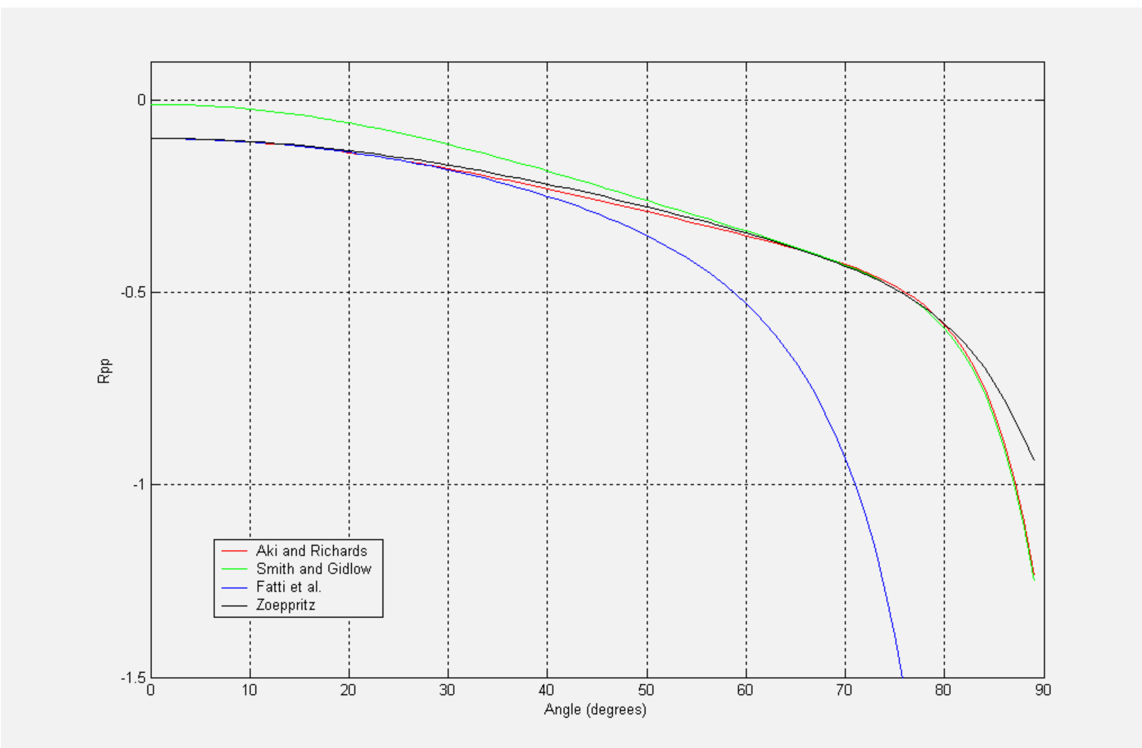

FIG. 5b. Class 3 (weak) R_{pp}.

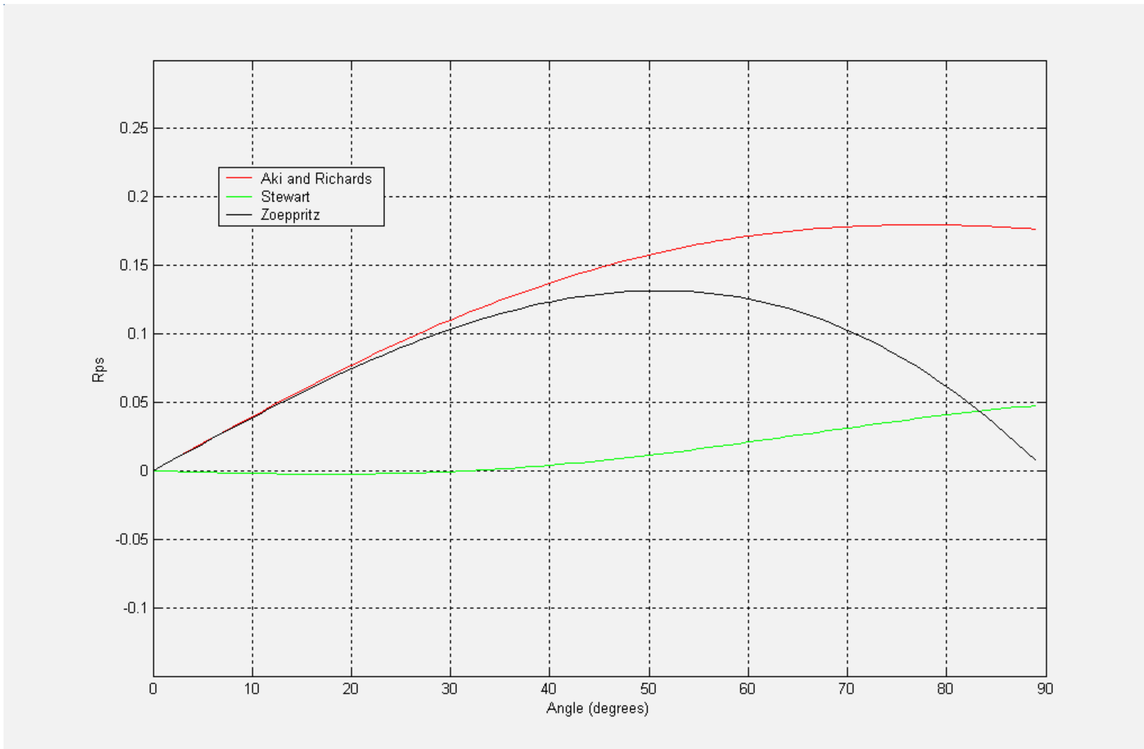

FIG. 6a. Class 3 (strong) R_{ps}.

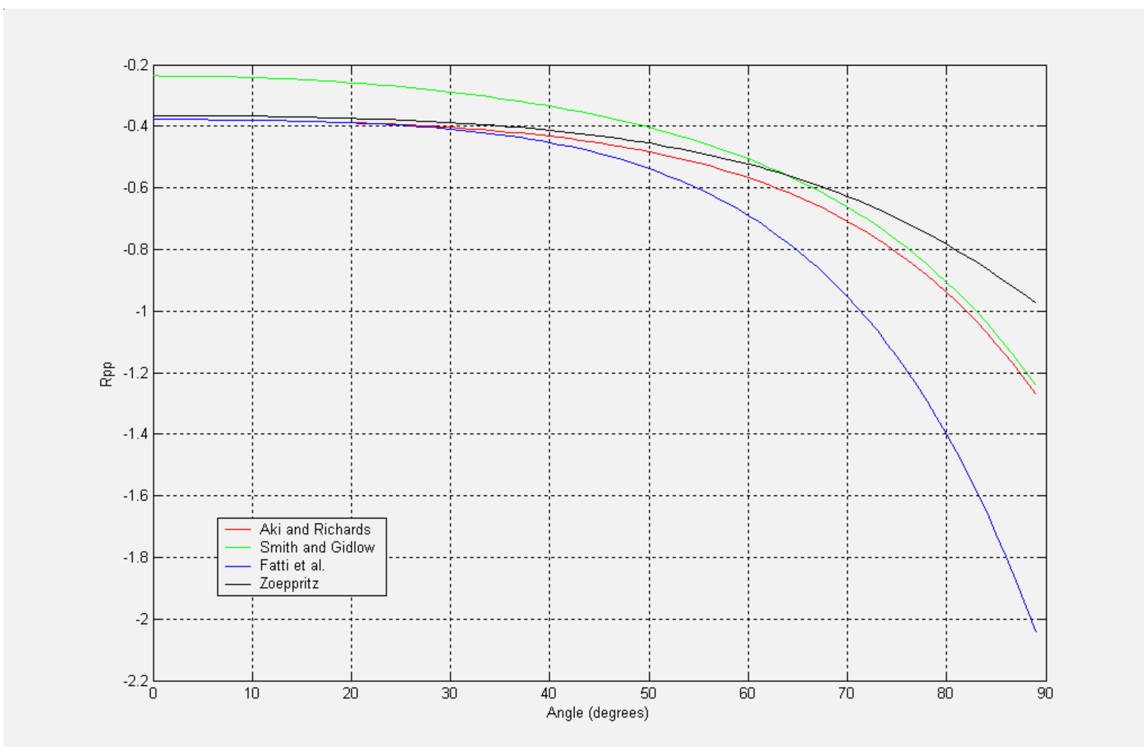

FIG. 6b. Class 3 (strong) R_{pp}.

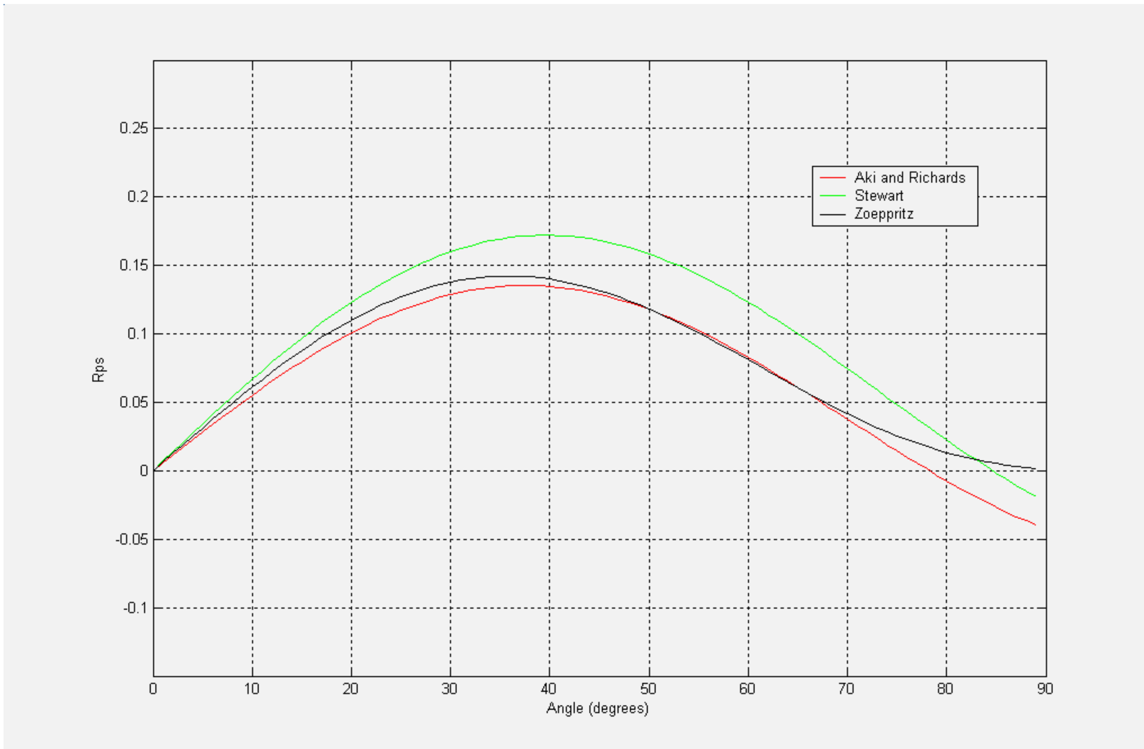

FIG. 7a. Class 4 (weak) R_{ps}.

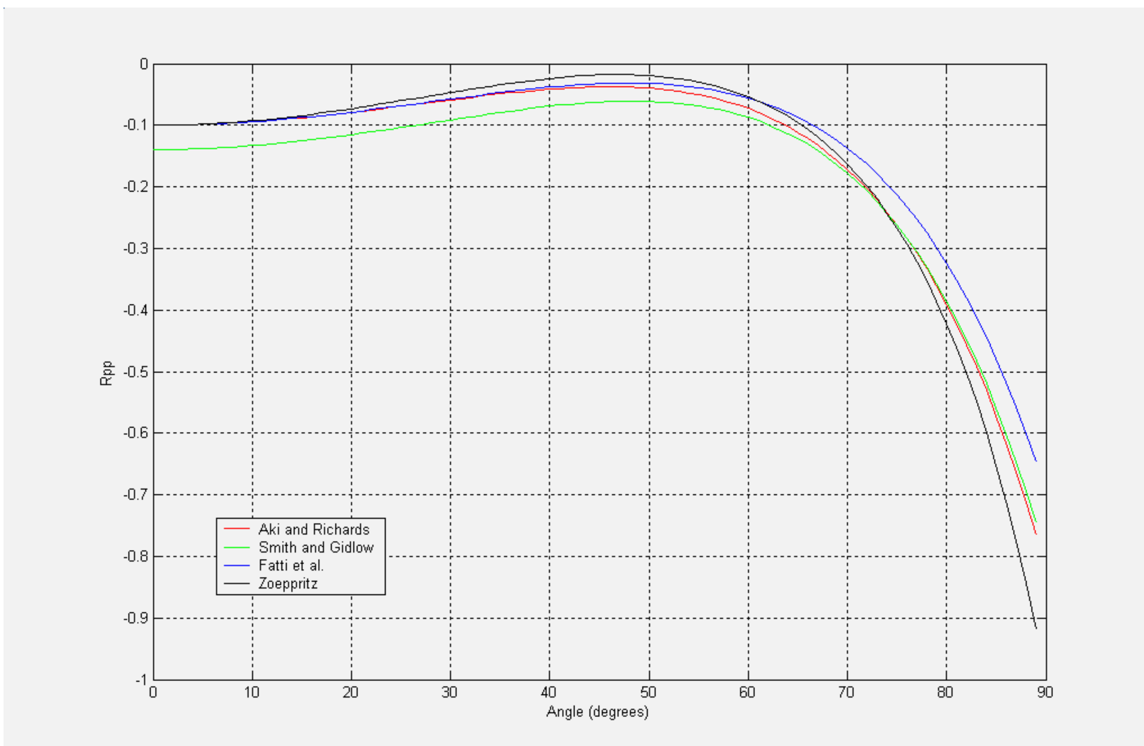

FIG. 7b. Class 4 (weak) R_{pp}.

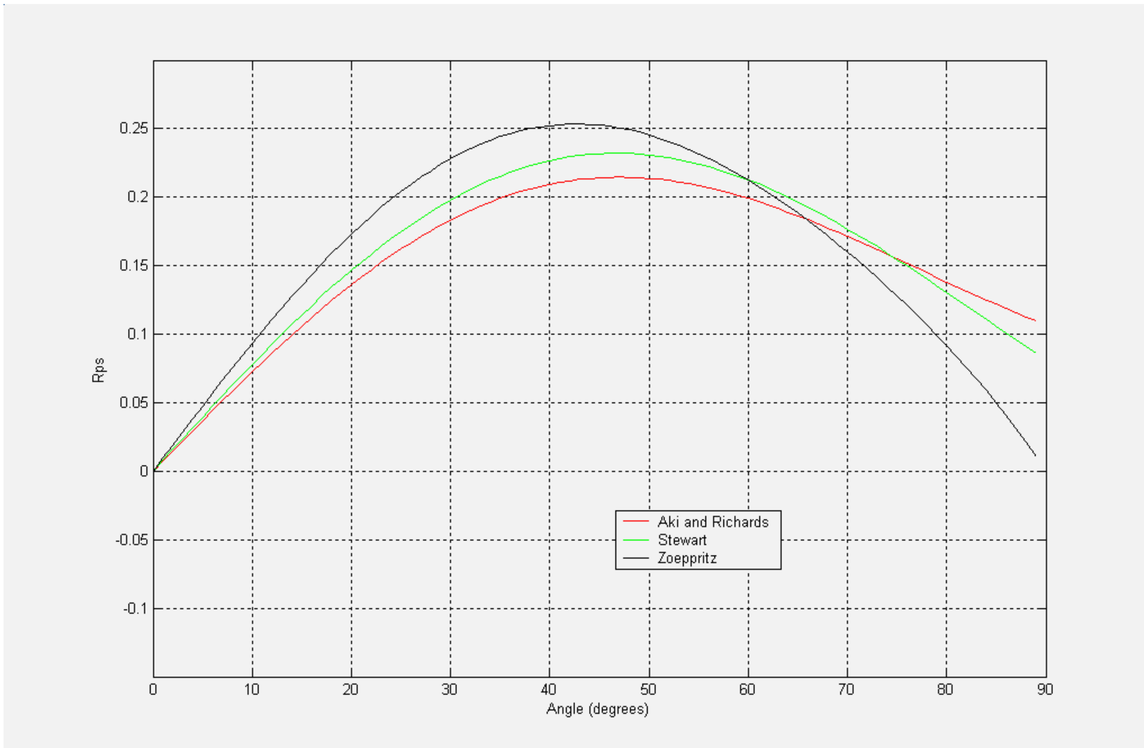

FIG. 8a. Class 4 (strong) R_{ps}.

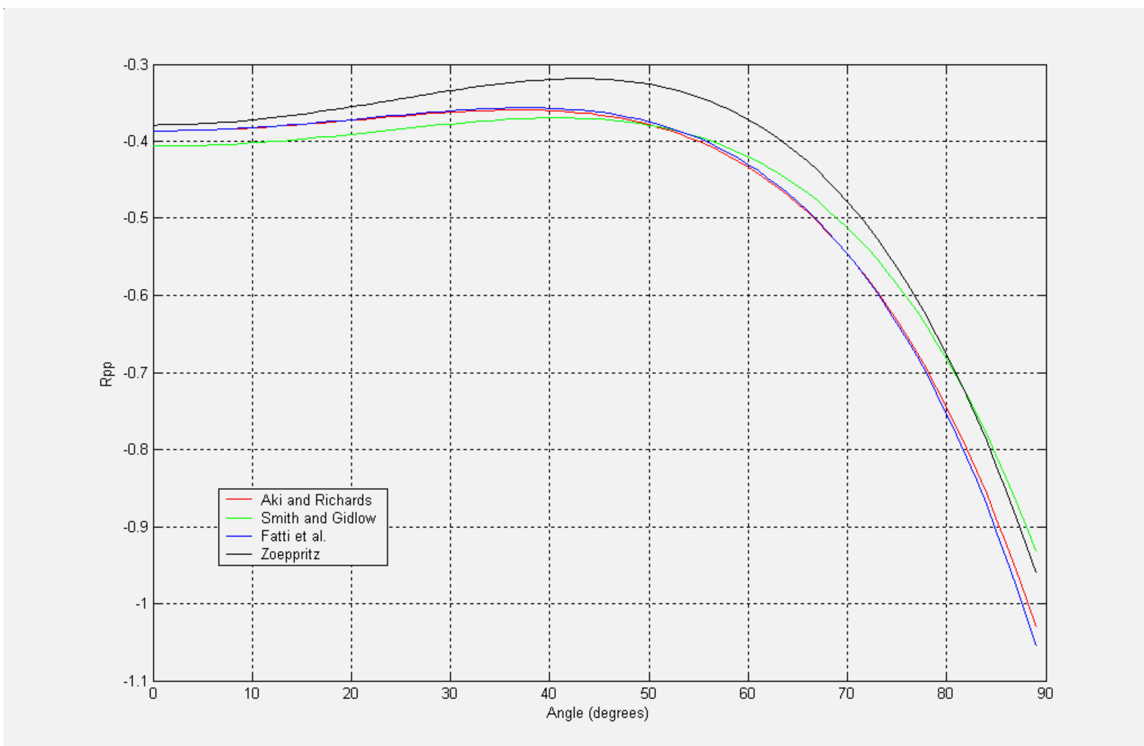

FIG. 8b. Class 4 (strong) R_{pp}.